

## Room Temperature Synthesis and Size Control of HKUST-1

by Gerardo Majano and Javier Pérez-Ramírez\*

Institute for Chemical and Bioengineering, Department of Chemistry and Applied Biosciences,  
ETH Zürich, Wolfgang-Pauli-Strasse 10, CH-8093, Zurich  
(fax: + 41 44 633 1405; e-mail: jpr@chem.ethz.ch)

Dedicated to Professor *Dieter Seebach* on the occasion of his 75th birthday

---

We report the synthesis of HKUST-1 ( $\text{Cu}_3(\text{btc})_2$ ; btc = benzene-1,3,5-tricarboxylate) and its growth kinetics by dynamic light scattering completely at room temperature without prior nucleation-induction steps. Upon an increase in concentration of the starting solutions, the generation of a pure phase requires adjustment of the  $\text{H}_2\text{O}/\text{EtOH}$  ratio. The presence of DMF is important to avoid competitive side phases. Replacement of DMF by a minimal amount of diethylamine resulted in the instantaneous formation of pure HKUST-1 upon mixing at room temperature. Additionally, the synthesis parameters strongly influence the final crystallite size and porous properties.

---

**Introduction.** – Metal-organic frameworks (MOFs), three-dimensional porous materials consisting of metal ions linked by organic molecules, provide a combination of very high surface areas, high metal dispersion, large pore size, and a high chemical flexibility. These features continue to spur their research for numerous applications, which have helped their transition from laboratory curiosities to large-scale production [1]. Since *Chui et al.* presented its synthesis and structure [2], HKUST-1 or  $\text{Cu}_3(\text{btc})_2$  (btc = benzene-1,3,5-tricarboxylate), which enjoys special attention due to its facile synthesis and stability, became the first of such materials to be scaled up through salt-free electrochemical route using copper electrodes by *BASF* as *Basolite C300* [1]. Aside from  $\text{CO}_2$ , methane, and  $\text{H}_2$  storage and separation applications [3][4], it has also recently shown activity in a growing number of *Lewis* acid catalyzed reactions such as *Friedländer* quinoline synthesis [5], isomerization of  $\alpha$ -pinene oxide [6], and the cyclization of citronellal [7].

For diverse applications, mainly sorptive and catalytic, the crystal size is an important factor which strongly influences the performance of the material, and its control and reduction may be of interest for other emerging applications. In the case of HKUST-1, an accurate control of crystallite dimensions is problematic due to *i*) fast crystallization kinetics and *ii*) constant nucleation. Numerous innovative synthesis variants have achieved a high degree of size control exploiting physical restrictions such as ‘location’ in electrochemical deposition and micropatterning [8] and ‘space confinement’ in microfluidics [9]. Other interesting approaches for size control comprise HKUST-1 growth on functionalized gold surfaces [10][11]. While these approaches certainly excel in controlling growth characteristics such as size, morphol-

ogy, and even crystal orientation, they are difficult to apply for bulk syntheses of crystals with reduced sizes.

As a general trend, HKUST-1 has shown a tendency to exhibit smaller crystallite size with lower temperatures or milder synthesis conditions. Whereas traditional synthesis at temperatures above 100° produce crystals larger than 20 µm [12], the bulk synthesis of HKUST-1 by refluxing in pure aqueous EtOH solution helped to generate small irregular crystals (< 10 µm) after 24 h [13]. Other approaches at lower temperature (40°) under ultrasound [14], or at higher temperature with microwave irradiation [15] have resulted in crystals with sizes around 1 µm, smaller than the traditional syntheses. Particularly small crystals (200 nm–2 µm) have been observed by *Zacher et al.* [16]. They have presented a complete study about the crystallization of HKUST-1 by skillfully inducing nucleation and crystallization at 85°, filtering the produced side phase, and analyzing the filtrate by time-resolved light scattering at room temperature. However, a bulk synthesis at room temperature by using this or similar formulations is complicated by the presence of side phases which consume starting material, thus limiting the final yield. Nevertheless, it is evident that the synthesis of HKUST-1 at room temperature would not only be beneficial for a generally easier process but also for a more accurate size control.

In this work, we present the successful room temperature synthesis of HKUST-1 using mainly concentrated solutions. In optimized syntheses, a generation of pure phase does not require any nucleation–induction step, and no side phase is present in any step of the crystallization. The influence of the composition as well as the influence of temperature on the phase purity and final crystal size is also studied.

**Results and Discussion.** – A precursor solution for HKUST-1, more concentrated than in typical bulk syntheses, was chosen as a starting point in order to enhance as much as possible the obtained yield. The investigated compositions and physicochemical properties are compiled in the *Table*. The higher concentration, such as in the case of *Zacher et al.* [16], has as immediate effect on the appearance of a side phase early in the crystallization process. Thus, it is not surprising to observe that sample *A*, as seen by X-ray diffraction, presents a side phase after 10-min stirring at room temperature which predominates even after 5 h (*Fig. 1, a*). Nevertheless, once the crystallization was

Table. Overview of HKUST-1 Compositions Investigated and Properties of the Obtained Products

Sample	Conditions	Molar composition 1 Cu <sup>2+</sup> /1 TA/... <sup>a)</sup>	Side-phase	Size [µm]	<i>S</i> <sub>BET</sub> [m <sup>2</sup> g <sup>-1</sup> ]	<i>V</i> <sub>micro</sub> [cm <sup>3</sup> g <sup>-1</sup> ]
A	25°, 5 h	12.9 DMF/34 EtOH/222 H <sub>2</sub> O	+	< 0.2	331	0.12
B	25°, 5 h	12.9 DMF/54 EtOH/200 H <sub>2</sub> O	+ <sup>b)</sup>	37	38	0.00
B-65	65°, 5 h	12.9 DMF/54 EtOH/200 H <sub>2</sub> O	–	> 40	899	0.34
C	25°, 5 h	12.9 DMF/80 EtOH/175 H <sub>2</sub> O	–	14	651	0.25
C-65	65°, 5 h	12.9 DMF/80 EtOH/175 H <sub>2</sub> O	–	40	1224	0.48
C-120	120°, 5 h	12.9 DMF/80 EtOH/175 H <sub>2</sub> O	–	> 40	1125	0.44
D	25°, 1 h	55 EtOH/220 H <sub>2</sub> O	+	< 0.2 <sup>c)</sup>	769	0.29
E	25°, 0 min	3.5 Et <sub>3</sub> NH/55 EtOH/220 H <sub>2</sub> O	–	0.18	940	0.33

<sup>a)</sup> Kept constant in all syntheses. <sup>b)</sup> Only side-phase. <sup>c)</sup> Irregular morphology and size distribution.

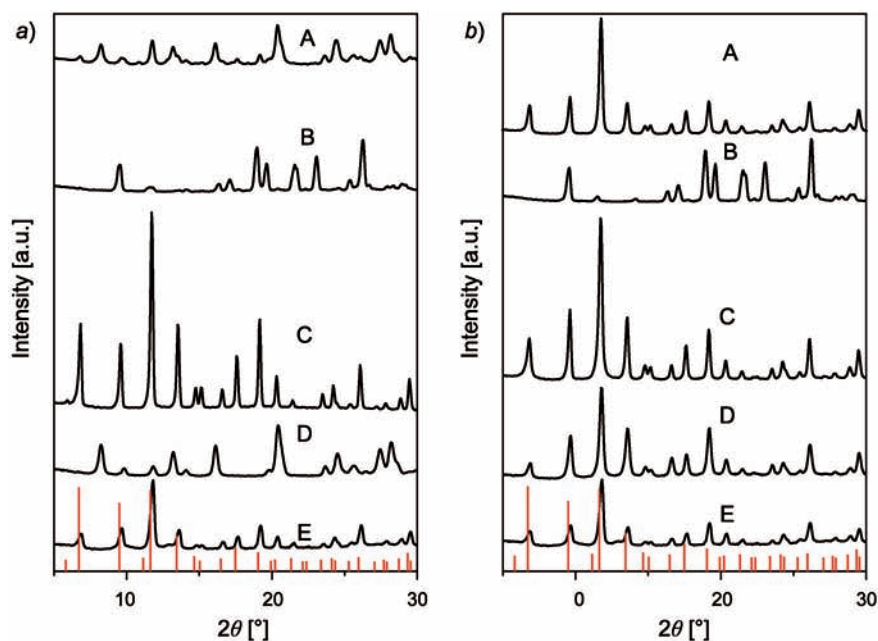


Fig. 1. XRD Diffraction patterns of samples A–E obtained at room temperature a) prior washing and b) after washing with EtOH. Theoretical HKUST-1 pattern as vertical lines.

stopped after 5 h, this phase turned out to be EtOH-soluble during filtration, and a certain amount of pure HKUST-1 was recovered (Fig. 1, b).

Taking into consideration that this phase was not only EtOH-soluble but also stabilized by H<sub>2</sub>O (*i.e.*, the phase did not dissolve after washing first with H<sub>2</sub>O and then with EtOH), it is most probably an oligomeric one or a two-dimensional form of Cu-btc. Such two-dimensional Cu-btc phases have previously been observed in hydrothermal syntheses [17][18]. This phase quickly turns the synthesis media into a thick gel and inevitably consumes all precursor species; thus, we attempted to prevent its formation by decreasing the H<sub>2</sub>O/EtOH ratio. And although we find a maximum in presence of side phase with sample B (H<sub>2</sub>O/EtOH 3.7), it completely disappears after decreasing the ratio to 2 in sample C (Fig. 1, a and b). The composition remains stable and produces pure HKUST-1 throughout the duration of the synthesis. A DMF-free synthesis of pure-phase HKUST-1 was not possible to be stabilized at room temperature. Nevertheless, pure HKUST-1 was recovered from sample D, synthesized in pure aqueous EtOH media, after dissolution of the side phase by EtOH washing. It is important to keep in mind that, with different molar compositions, rather different side phases were observed, as observed comparing samples A and B (Fig. 1, a). This indicates that, in order to attain a side phase-free crystallization using a certain concentration, the H<sub>2</sub>O/EtOH ratio has to be modified accordingly.

While the elimination of DMF is highly desired (due to its carcinogenic and teratogenic character), the general trend reported by Khan and Jung [14] also strongly influenced our experiments, where the formation of HKUST-1 exhibits a

maximum of surface area at a certain DMF concentration and declines upon increase or decrease of it. The neat formation of HKUST-1 expressed as  $3 \text{ Cu}(\text{NO}_3)_2 + 2 \text{ H}_3\text{btc} \rightarrow \text{Cu}_3(\text{btc})_2 + 6 \text{ HNO}_3$  would profit from the basic character of DMF by activating the trimesic acid (= benzene-1,3,5-tricarboxylic acid) and favoring HKUST-1 formation by stabilizing the produced proton, which would explain the results reported by *Chui* about room temperature crystallization in pure DMF [2]. Nevertheless, in our case, the addition of just the amount of DMF theoretically required to activate the trimesic acid was not successful in producing pure phase at room temperature in aqueous ethanolic solution, and, thus, more complicated solvent effects should play an important role in the generation of three-dimensional Cu-btc structure. However, the direct deprotonation of trimesic acid and subsequent formation of HKUST-1 was achieved by using  $\text{Et}_2\text{NH}$  instead of DMF that has a  $\text{p}K_{\text{b}}$  value of 2.9 compared to DMF, which is rather a polar organic solvent in aqueous media (sample *E*). The less intense reflections in the diffraction pattern is due to the reduced size of the crystals (*vide infra*). In this case, the formation of pure-phase HKUST-1 occurred instantaneously during addition of the  $\text{Cu}(\text{NO}_3)_2$  solution to the deprotonated trimesic acid solution at room temperature (*Fig. 1* and *Table of Contents* image). The crystallization was quantitative, and no copper was detected by UV/VIS spectrometry of the filtrates.

The disappearance of the side phase in sample *C* enabled the undisturbed monitoring of the crystallization by dynamic light scattering (DLS) without the need of any prior nucleation/crystallization or filtration steps (*Fig. 2*). The crystallization evolution of sample *C*, monitored *in situ* by DLS, interestingly follows the results obtained by *Zacher et al.* [16], where HKUST-1 solutions proceed to generate rapidly 200-nm crystals after a few minutes at room temperature. The crystallization remains constant for *ca.* 5–10 h, when the generation of large crystals begins. After 15 h, the size of the crystals surpasses the limits of detection of DLS (*ca.* 3  $\mu\text{m}$ ) and start to precipitate from the solution. It is also interesting to note that at room temperature, albeit slow, the crystallization speed remains constant as evidenced by the continuing

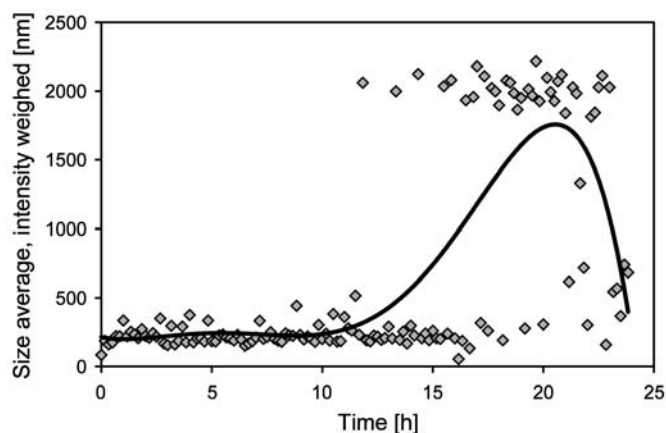


Fig. 2. Size evolution of sample *C* at room temperature obtained by DLS measurements during 24 h under static conditions. Black line represents the polynomial trend of the size.

crystallization of the filtrates during several days, which yielded particle size and distribution similar to the product isolated after 5 h.

The similarity of our results to those of *Zacher et al.* [16] may well be due to the fact that, in pure aqueous EtOH solutions, the side phase would unevenly consume a great part of the starting materials. After its filtration, a completely new diluted composition would be obtained which would not only favor the formation of HKUST-1 but also contain small crystals of pure HKUST-1. The latter can jump-start further crystallization. Nevertheless, the stability of such a diluted medium for producing pure phase after the reported 2 h still remains an open question.

The crystal size, as determined with the help of scanning electron microscopy, (SEM; *Fig. 3*), reveals the effect of room temperature in slowing down crystal growth, and thus final size and morphology. While small (14  $\mu\text{m}$ ) octahedral crystals were obtained from room temperature syntheses, large ones  $> 40 \mu\text{m}$  were already present at 65°. Furthermore, the morphology is unexpectedly well-defined at lower temperature but varies from the ideal octahedral shape at 65° and 120°. It was interesting to observe that, throughout all the samples, there is a dissolution–recrystallization occurring after an ideal crystallization time has been reached, in our case 5 h, resulting in a decreased definition of crystalline features and generation of smaller crystals, as seen in *Fig. 3, d*. The difference of this process from the typical *Ostwald* ripening may be due to the contribution of constant nucleation inherent in HKUST-1 media, which would stabilize small crystals. Although ignored, this effect can sometimes be observed in the open literature as partially corroded crystals with other smaller crystals present [19][20].

Upon crystallization at higher temperatures, compositions, which otherwise favored formation of lower-dimensional Cu-btc side phases at room temperature such as sample *D*, yielded pure HKUST-1 (see *Supplementary Information*, *Fig. SI1*<sup>1)</sup>) with unusual crystallite shapes derived from the octahedral morphology such as elongated plates to hexagons and triangles with a higher aspect ratio (*Fig. 3, e*). This suggests an aggregation of lower-dimensional secondary building units or crystals into a three-dimensional structure as a plausible formation mechanism, resulting in a more plate-like morphology. Finally, a predictably smaller size around 180 nm (*Fig. 3, f*) was observed in the sample synthesized with Et<sub>2</sub>NH at room temperature (sample *F*). Crystals above this size had clear faceted features, while smaller ones were basically spherically shaped. The small size would be caused by the rapid crystal formation and is expected to vary with the addition speed of the copper solution and stirring speed during addition, which were fixed in our study.

Through nitrogen sorption measurements, it is evident that the porous and sorptive properties of HKUST-1 are strongly influenced by the change in size and morphology (*Table* and *Fig. 4*). The microporosity increases with the increase in crystal size and better defined morphologies, as seen in sorption isotherms of samples *A* and *C*. Sample *E* shows a surprisingly high microporosity in spite of the fast crystallization time and small crystal size. The reduction in size contributes also to the generation of textural porosity which is absent in samples with larger crystallites such as in the commercial HKUST-1, *Basolite C300*. Predictably, upon increasing the synthesis

---

<sup>1)</sup> *Supplementary Information* is available from the corresponding author.

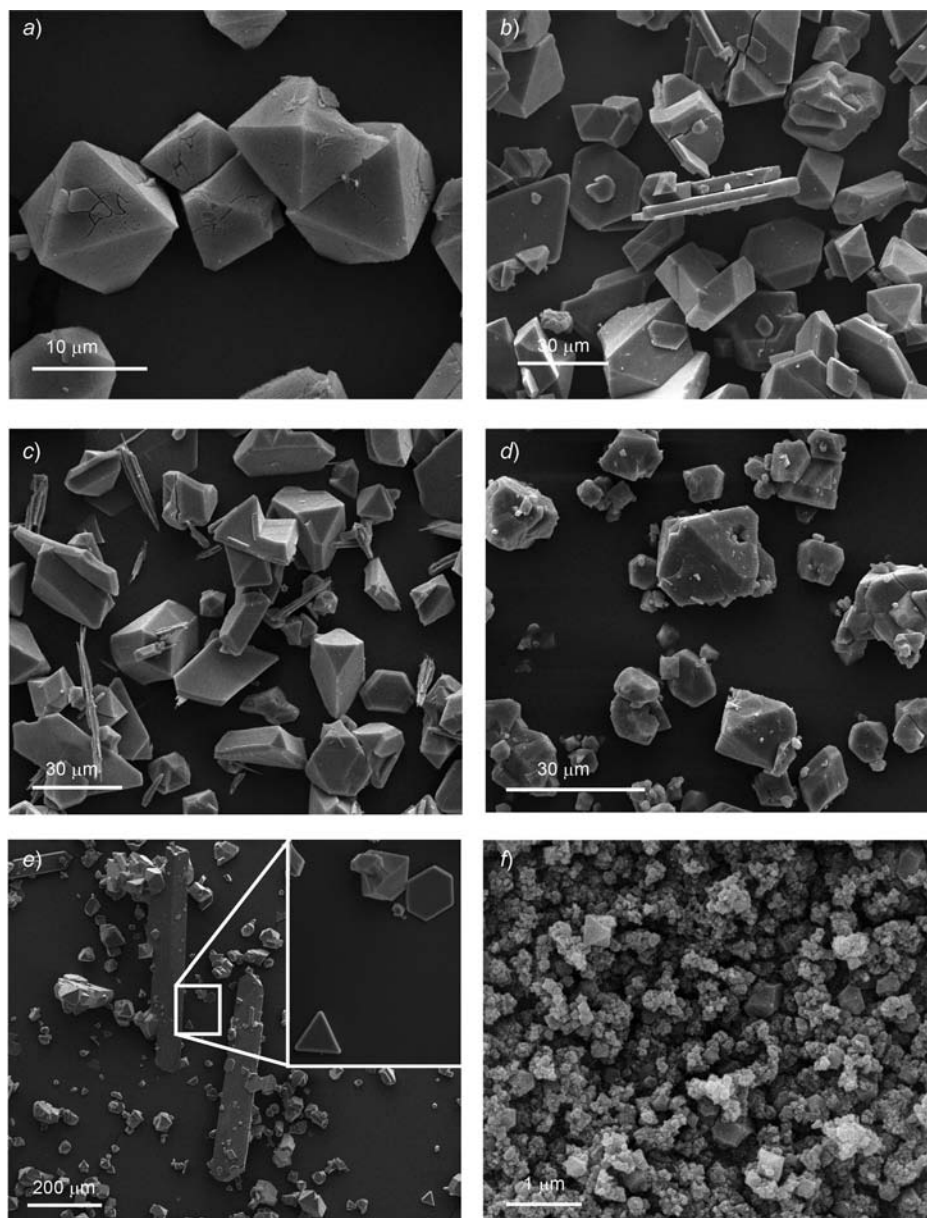


Fig. 3. SEM Images of samples a) C, b) C-65, and c) C-120 after 5 h, synthesis and d) C after 1 day and e) sample B-65 and f) sample E immediately after mixing at room temperature

temperature above 25°, this textural porosity disappears as seen in the sample C synthesized at 65° and 120° (Fig. 4, b). The small decrease in surface area at 120° is most probably caused by the sample surpassing the ideal crystallization time and suffering of the aforementioned dissolution–recrystallization process.

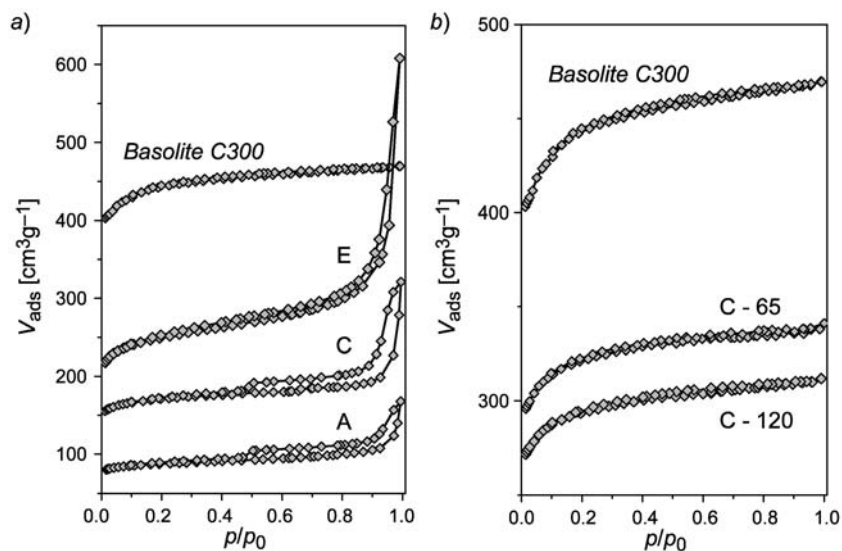


Fig. 4. Nitrogen isotherms of samples obtained a) at room temperature, and b) at 65° and 120° compared to commercial Basolite C300

The thermal stability of the obtained materials remained largely unaffected and was in the expected range for conventional HKUST-1. Fig. 5 shows the onset of the thermal decomposition starting after 300° for all the samples studied at 25° and higher synthesis

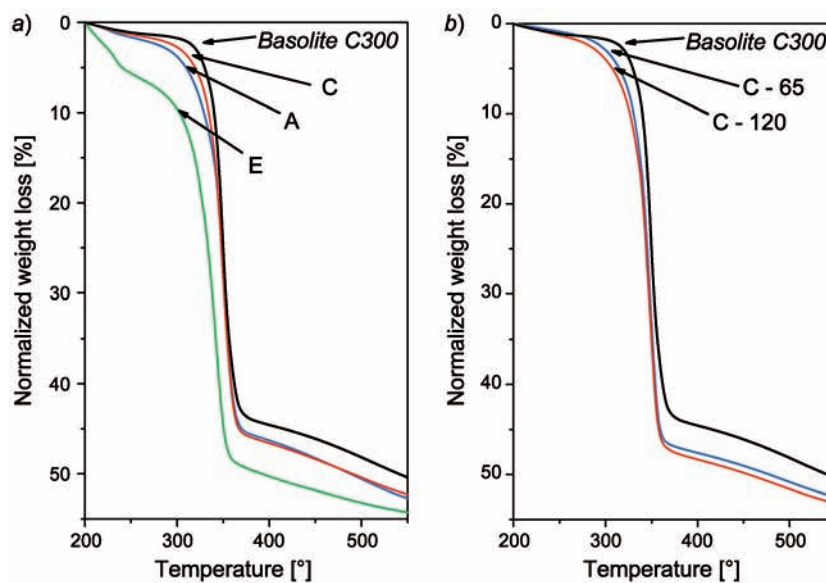


Fig. 5. TGA Profiles of representative samples obtained a) at room temperature, and b) at 65° and 120° after 5 h compared to commercial Basolite C300

temperatures. The exception was sample *E*, which shows a minimal decrease of a few degrees centigrade in the onset of the decomposition, which is in line with the extremely short time the sample required for crystallization and resulting in smaller crystal size. Larger crystals produced at 65° and 120° are also directly in line with the commercial *Basolite C300* sample and show identical decomposition onsets.

**Conclusions.** – We have presented a complete study of HKUST-1 crystallization exclusively at room temperature with the help of solutions containing a low amount of DMF, fit for laboratory-scale synthesis. By careful tuning of the solvent concentration and H<sub>2</sub>O/EtOH ratio, we thus increase the crystallization speed while avoiding side-phase formation. Due to the stabilizing nature of DMF during synthesis, DMF-free formation of HKUST-1 was not possible in pure aqueous EtOH media at room temperature. However, minimal amounts of Et<sub>2</sub>NH resulted in an unprecedented fast crystallization of nano-sized HKUST-1 crystals upon mixing at room temperature. We thus established the importance of the compositional factor of the starting solutions on controlling size and crystallization behavior at room temperature. It should also be noted that, even using these mild conditions, the formation of HKUST-1 suffers from a temperature- and composition-dependent dissolution–recrystallization process which affects the final morphological and, most importantly, porous features.

#### Experimental Part

*Synthesis of HKUST-1.* In all of the syntheses, an aq. soln. of Cu(NO<sub>3</sub>)<sub>2</sub>·3 H<sub>2</sub>O (*Aldrich*, > 98%) was added under stirring to a soln. of trimesic acid (= benzene-1,3,5-tricarboxylic acid; *ACBR*, 98%) in EtOH (and DMF, *Aldrich*, > 99.8%; or Et<sub>2</sub>NH; *AlfaAesar*, 99+%, if applicable). The soln. was stirred at r.t. for 1 to 24 h. For syntheses above 100°, the clear solns. were transferred to *Teflon*-lined steel autoclaves. The product was isolated by filtration and dried at 65°. The compositions and specific synthesis conditions are compiled in the *Table*.

*Characterization.* The crystallinity and phase purity of the samples were determined by X-ray powder diffraction using a *PANalytical X'Pert Pro* diffractometer in *Debye–Scherrer* geometry with CuK<sub>α</sub> radiation. Scanning electron microscopy (SEM) images were obtained with a *FEI Quanta 200* microscope. The size evolution of selected samples was followed in static conditions at 20° using dynamic light scattering (DLS) on a *Malvern Nanosizer* instrument (He-Ne laser 633 nm). Porous properties were probed using a *Quantachrome SI* nitrogen sorption instrument after degassing the samples for 16 h at 150°. Thermogravimetric measurements were carried out in a *Mettler Toledo STAR<sup>c</sup> TGA* instrument under a flow of air (40 cm<sup>3</sup> min<sup>-1</sup>) and a heating rate of 10° min<sup>-1</sup>.

We would like to thank Dr. *Karsten Kunze* and Mr. *Peter Wägli* (Electron Microscopy ETH Zurich, EMEZ) for their help with SEM imaging, and *Bastian Brand* for his kind help with DLS measurements.

#### REFERENCES

- [1] A. U. Czaja, N. Trukhan, U. Müller, *Chem. Soc. Rev.* **2009**, *38*, 1284.
- [2] S. S.-Y. Chui, S. M.-F. Lo, J. P. H. Charmant, A. G. Orpen, I. D. Williams, *Science* **1999**, *283*, 1148.
- [3] B. Panella, M. Hirscher, H. Pütter, U. Müller, *Adv. Funct. Mater.* **2006**, *16*, 520.
- [4] J. R. Karra, K. S. Walton, *J. Phys. Chem. C* **2010**, *114*, 15735.
- [5] A. Sachse, R. Ameloot, B. Coq, F. Fajula, B. Coasne, D. De Vos, A. Galarneau, *Chem. Commun.* **2012**, *48*, 4749.



- [6] L. Alaerts, E. Séguin, H. Poelman, F. Thibault-Starzyk, P. A. Jacobs, D. E. De Vos, *Chem. – Eur. J.* **2006**, *12*, 7353.
- [7] L. Alaerts, F. Thibault-Starzyk, E. Séguin, J. F. M. Denayer, P. A. Jacobs, D. E. De Vos, *Stud. Surf. Sci. Catal.* **2007**, *170*, 1996.
- [8] R. Ameloot, E. Gobechiya, H. Uji-i, J. A. Martens, J. Hofkens, L. Alaerts, B. F. Sels, D. E. De Vos, *Adv. Mater.* **2010**, *22*, 2685.
- [9] D. Witters, N. Vergauwe, R. Ameloot, S. Vermeir, D. De Vos, R. Puers, B. Sels, J. Lammertyn, *Adv. Mater.* **2012**, *24*, 1316.
- [10] E. Biemmi, C. Scherb, T. Bein, *J. Am. Chem. Soc.* **2007**, *129*, 8054.
- [11] O. Shekhah, H. Wang, S. Kowarik, F. Schreiber, M. Paulus, M. Tolan, C. Sternemann, F. Evers, D. Zacher, R. A. Fischer, C. Wöll, *J. Am. Chem. Soc.* **2007**, *129*, 15118.
- [12] K. Schlichte, T. Kratzke, S. Kaskel, *Microporous Mesoporous Mater.* **2004**, *73*, 81.
- [13] J. Kim, S.-H. Kim, S.-T. Yang, W.-S. Ahn, *Microporous Mesoporous Mater.* **2012**, *161*, 48.
- [14] N. Abedin Khan, S.-H. Jhung, *Bull. Korean Chem. Soc.* **2009**, *30*, 2921.
- [15] Y.-K. Seo, G. Hundal, I. T. Jang, Y. K. Hwang, C.-H. Jun, J.-S. Chang, *Microporous Mesoporous Mater.* **2009**, *119*, 331.
- [16] D. Zacher, J. Liu, K. Huber, R. A. Fischer, *Chem. Commun.* **2009**, 1031.
- [17] J. Chen, T. Yu, Z. Chen, H. Xiao, G. Zhou, L. Weng, B. Tu, D. Zhao, *Chem. Lett.* **2003**, *32*, 590.
- [18] J. Gascon, S. Aguado, F. Kapteijn, *Microporous Mesoporous Mater.* **2008**, *113*, 132.
- [19] S. Marx, W. Kleist, A. Baiker, *J. Catal.* **2011**, *281*, 76.
- [20] P. Chowdhury, C. Bikkina, D. Meister, F. Dreisbach, S. Gumma, *Microporous Mesoporous Mater.* **2009**, *117*, 406.

Received August 14, 2012